Study on Current–Voltage Curves of Composite Bipolar Membrane for Water and Methanol Solutions

TZU-JEN CHOU,[1] PO-DA HONG,[1] AKIHIKO TANIOKA[2]

[1] Graduate School of Textile and Polymer Engineering, National Taiwan University of Science and Technology, Taipei 10607, Taiwan

[2] Department of Organic and Polymeric Materials, Tokyo Institute of Technology, Tokyo 152, Japan

Received 16 March 1999; accepted 1 July 1999

ABSTRACT: The current–voltage curves of a composite bipolar membrane (CBM) were experimentally measured by inserting the thin poly(acrylonitrile) (PAN) membrane between cation- and anion-exchange membranes for water and methanol solutions. In each solution system, 0.05 mol/L LiCl was used as the electrolyte. The measured results show that the thin PAN membranes enhanced the water- and methanol-splitting effect. This phenomenon can be explained by the protonation–deprotonation reactions occurring between the functional group of PAN (—C≡N, cyano) and the water or methanol molecules in the intermediate region of the CBM. The effect of niobium alloy (Nb_3Ga), fullerene (C_{60}) and titanium oxide (TiO_2) existing in the intermediate region of the CBM was also experimentally examined in this study. It was found that the effect of these compounds on water or methanol-splitting was not obvious. © 2000 John Wiley & Sons, Inc. J Appl Polym Sci 75: 1597–1604, 2000

Key words: current–voltage curves; composite bipolar membrane; solvent splitting; membrane interface

INTRODUCTION

The characterization of bipolar membranes has been carried out for aqueous solution systems by studying the current–voltage curves,[1–8] membrane potentials[9–14] and AC impedance spectra.[15–17] One of the main interests in bipolar membranes is their water-splitting property. Water splitting has to be accompanied by water dissociation into hydrogen and hydroxide ions at the boundary surface between anionic and cationic layers and successive ion diffusion through charged layers. Ohki[18] predicted the rectification effect by consideration of the Donnan equilibrium and the Nernst–Planck equation. Mafé and coworkers[1–3,6] theoretically derived an equation to explain the experimental results of the current–voltage curve for different bipolar membranes at different temperatures. In their deduction, the water-splitting phenomenon was accounted for by means of either the Onsager theory of the second Wien effect[19] or the chemical reaction model.[29] However, the coupling of water splitting with ion transport is still poorly understood from the viewpoints of basic materials science, chemistry, and physics.

A composite bipolar membrane (CBM) consisting of a layered structure involving a cation-selective membrane joined to an anion-selective membrane is used for the analysis, because the physicochemical properties of both monopolar membranes (water content, fixed charge density and ionic mobility ratio) can be separately ob-

Correspondence to: P.-D. Hong (phong@hp730.tx.ntust.edu.tw).

Journal of Applied Polymer Science, Vol. 75, 1597–1604 (2000)

Table I Physicochemical Properties of the Studied Ion-Exchange Membranes

Membrane	Thickness (mm)	Water Content (wt %)	Fixed Charged Density (mol/L)
K-101	0.22	27	5.0
A-201	0.23	26	4.2

tained. In the previous paper,[21] methanol splitting was observed in the case of LiCl-methanol solution because of its somewhat large autoprotolysis constants. In this study, the current–voltage curves of the CBM were measured by inserting the thin poly(acrylonitrile) (PAN) membrane between the cation- and anion-exchange membranes for the water and methanol solutions in order to examine the water and methanol splitting affected by the membrane interface component. In each solution system, 0.05 mol/L LiCl was used as the electrolyte. The effect of Nb_3Ga, C_{60}, and TiO_2 existing in the intermediate region of the CBM also was experimentally examined. These components were chosen just because of their specific structures. The experiment was a new attempt to find out the available component that can enhance the splitting of water and methanol.

EXPERIMENTAL

Samples

A cation-exchange membrane (K-101; Asahi Chemicals), which is composed of poly(divinylbenzene-*co*-styrene) containing sulfonic acid groups in a polymer matrix, and an anion-exchange membrane (A-201; Asahi Chemicals), which is composed of poly(butadiene-*co*-styrene) containing quaternary amino groups in a polymer matrix, were used for the measurements. Both membranes were supported by woven polymer fiber cloth in order to prevent the swelling caused by the organic solvents. The thickness, water content, and fixed charge density of both membranes that were measured and offered by the manufacturer are given in Table I. Prior to the measurements being carried out, both membranes were immersed in 3 mol/L LiCl aqueous solution for 3 days to ensure that the counter-ions were exchanged for the same species. After both membranes were washed thoroughly with ion-exchanged water, they were immersed in ion-exchanged water for 3 days to remove the excess ions in the membrane matrices. Finally, both membranes were immersed in water or methanol solvents for a week to ensure that the solvents were sorbed in the membrane phase. The CBM, which consisted of a layered structure involving K-101 joined to A-201, was used for the measurement of the current–voltage curves in this study.

A mixed solution of 15 wt % PAN (Mitsubishi Rayon) in dimethylformamide was stirred at 70°C for 5 h and was subsequently cooled to 25°C. Nb_3Ga, C_{60}, or TiO_2 powder was added to the solution and cast onto a glass plate (15 cm $\times$ 10 cm) guided by a 100 μm thick spacer. After the solvent was evaporated for 10 min at 25°C, the plate was immersed in water or methanol for 1 h. The membrane was removed from the plate and immersed in 0.05 mol/L LiCl water or methanol solution for 1 day to remove dimethylformamide. The concentration of Nb_3Ga, C_{60}, and TiO_2 was 0.1 g/g dry membrane, and the thickness of the membranes was 67 μm. The compounds used in this study were as follows: none for the membrane M1, Nb_3Ga for the membrane M2, C_{60} for the membrane M3, and TiO_2 for the membrane M4. These membranes were inserted between the charged membranes K-101 and A-201 to examine the effect of interface component on current–voltage characteristic.

Measurement

The current–voltage curves under reverse bias conditions across the CBM were measured by inserting the thin PAN membrane between the cation- and anion-exchange membranes for 0.05 mol/L LiCl water and methanol solutions at 30.0 $\pm$ 0.1°C. Figure 1 shows a schematic diagram of the current–voltage measurement apparatus. The CBM was placed between two electrodialytic half-cells. When the entire electrodialysis cell was reverse-biased using the working electrodes, the large electric field appearing at the CBM junction produced an excess of cations and anions due to the electric field-enhanced solvent dissociation reaction. These ions permeated the corresponding ion-exchange layers of the CBM and entered the adjacent solutions. The micro tube pumps (EYELA, MP-3) maintained a continuous cyclic flow of the solutions to ensure that the concentration of LiCl in the electrodialysis cell was the same during the measuring period.

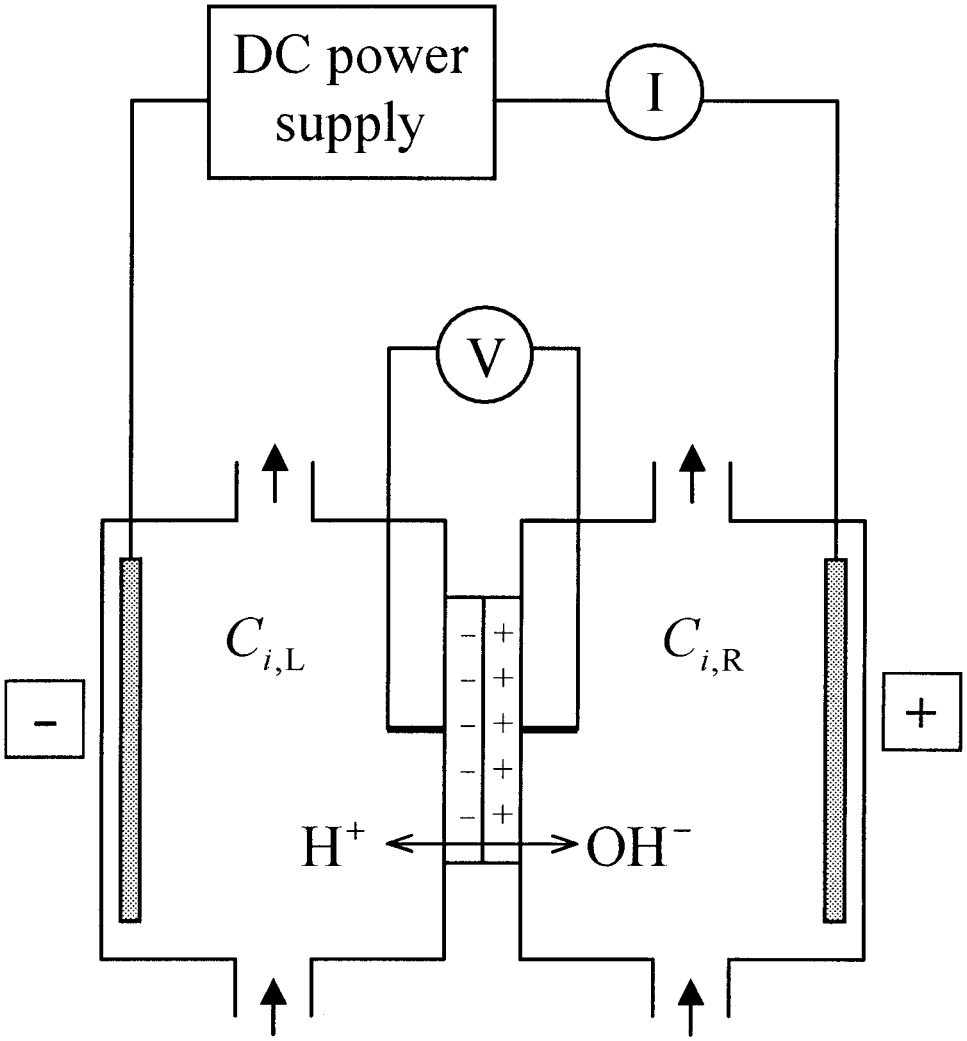

Figure 1 Schematic diagram of current–voltage measurement apparatus.

Before the actual experiment, all compartments were filled with the corresponding solutions for a couple of hours in order to produce an equilibrium state between the CBM and the solutions. The current–voltage curves were obtained by applying a potential difference to the system via a DC signal source (7011; HIOKI) and allowing the current to reach a steady state. Nickel (cathode) and platinum (anode) electrode plates were used. The potential drop across the CBM was measured using two Ag/AgCl electrode wires (diameter, 1.0 mm) that were laid on both surfaces of the CBM and connected to a digital voltmeter (7011; HIOKI). Special care was taken in placing these Ag/AgCl electrode wires close to the CBM surfaces in order to minimize the ohmic potential drops in the bulk solutions. Prior to the measurements being carried out, the effect of the bulk solutions on the ohmic drops was examined. In this case, the resistance from the bulk solutions was below 0.1% of the total resistance. Also, the distances between the Ag/AgCl electrode wires and the CBM surfaces were kept approximately constant during all the experimental runs. Under reverse bias conditions, the current and voltage are definitely negative values, which appear in the third quadrant. However, in this work, the measured current and voltage were multiplied by -1 in order to have them appear in the first quadrant.

RESULTS AND DISCUSSIONS

The experimental results for the current–voltage curves of the CBM installed with M1 and nothing

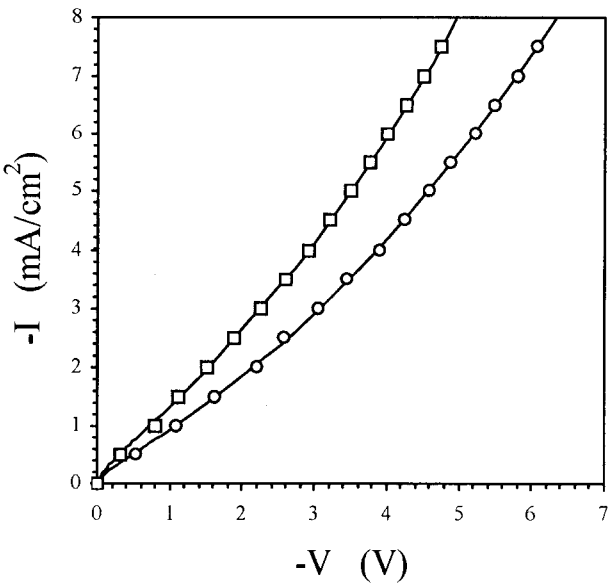

Figure 2 Current–voltage curves of the CBM for water-LiCl solution. The curves have been measured by inserting the membranes M1 (□) and nothing (○) in the intermediate region of the CBM. Solid lines show the calculated results.

in the intermediate region in the 0.05 mol/L LiCl water solution are shown in Figure 2. As previously described, the measured current and voltage were multiplied by −1 in order to have them appear in the first quadrant. In Figure 2, the electric field-enhanced dissociation can be observed for sufficiently high applied voltages, and the water-splitting effect is enhanced by inserting the thin PAN membrane in the intermediate region of the CBM. Ordinary water dissociation cannot explain the magnitude of the electric current. It is generally believed that the H^+ and OH^- ions originate in a very thin region at the interface between the two ion-exchange layers. Nevertheless, it is not known exactly which mechanism is responsible for this enhanced dissociation.

One possible explanation was suggested by Wien and Schile.[22] They pointed out that the ion mobility increases with increasing electric field in weakly dissociated electrolytes. This effect has been called the second Wien effect, and the theory was developed by Onsager.[19] Water is a weakly dissociated electrolyte; thus, this theory can be applied to a bipolar membrane. A high electric field is generated at the space charge region with a p-n junction. Because the structure of the bipolar membrane resembles that of a semiconductor, such a high electric field may be produced. Onsager's theory considers an exponential dependence of the water dissociation rate on the electric field and assumes that the water recombination rate remains unaffected. However, Mafé and Ramírez have pointed out that some limitations exist in this model, and these limitations will cause the model to fail in some systems.[6]

Simons[20] suggested that the H^+ and OH^- ions may be generated from protonation–deprotonation reactions between some functional groups and the water molecules and proposed the following mechanism for the water dissociation reaction

$$B + H_2O \rightleftharpoons BH^+ + OH^-$$

$$BH^+ + H_2O \rightleftharpoons B + H_3O^+ \qquad (1)$$

where BH^+ refers to the catalytic active center for the proton transfer reactions. There are two reasons why the proton transfer reaction accelerates the water splitting at bipolar membranes. The first is the influence of the electric field, which causes the orientation of the water molecules to assume an optimum position for the reaction with a functional group. The second is the influence of the counter ion on the functional group in the space charge region. The concentration of the counter ion is very low in this region, because it is extracted from the membrane to an electrode. Therefore, the functional group without a counter ion simultaneously reacts with water, as shown in Eq. (1).

The experimental results for the current–voltage curves of the CBM installed with M1 and nothing in the intermediate region in the 0.05 mol/L LiCl methanol solution are shown in Figure 3. The results show that the electric field-enhanced dissociation existed for sufficiently high applied voltages, and the methanol-splitting effect is enhanced by inserting the thin PAN membrane in the intermediate region of the CBM. The phenomenon can be explained by the belief that the H^+ and CH_3O^- ions may be generated from protonation–deprotonation reactions between the functional group and the water molecules, which have similar mechanism[21] to Eqs. (1)

$$B + CH_3OH \rightleftharpoons BH^+ + CH_3O^-$$

$$BH^+ + CH_3OH \rightleftharpoons B + CH_3OH_2^+ \qquad (2)$$

Figures 4 and 5 show the experimental results for the current–voltage curves of the CBM installed with M1, M2, M3, and M4 in the intermediate

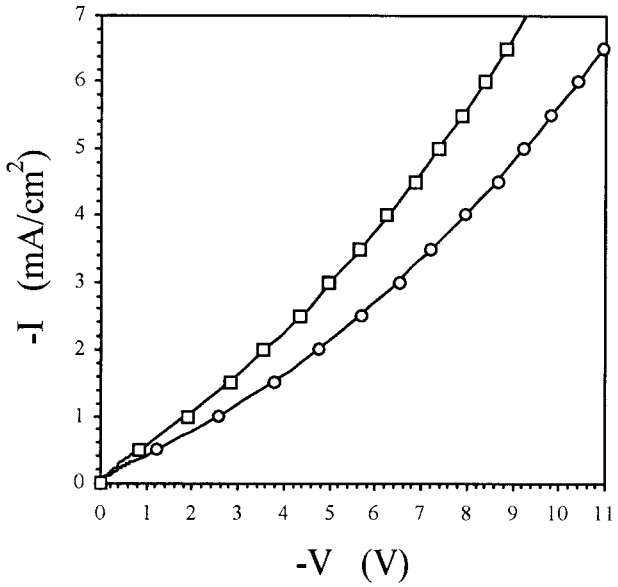

Figure 3 Current–voltage curves of the CBM for methanol-LiCl solution. The curves have been measured by inserting the membranes M1 (□) and nothing (○) in the intermediate region of the CBM. Solid lines show the calculated results.

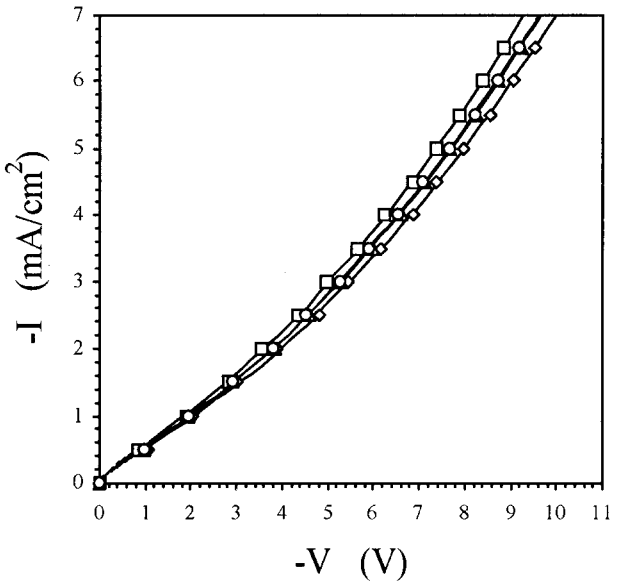

Figure 5 Current–voltage curves of the CBM for methanol-LiCl solution. The curves have been measured by inserting the membranes M1 (□), M2 (◇), M3 (△), and M4 (○) in the intermediate region of the CBM. Solid lines show the calculated results.

region in the 0.05 mol/L LiCl water and methanol solution, respectively. These figures show that the presence of Nb_3Ga, C_{60}, and TiO_2 obviously does not increase the solvent-splitting effect. They can be seen as some impurities in the PAN membrane. One of the reasons may be that the measurements were done at low temperature; thus, catalysis by these compounds obviously cannot be observed.

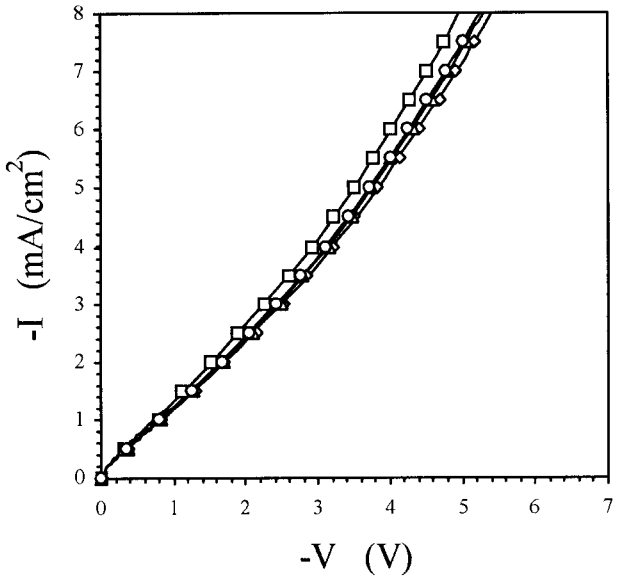

Figure 4 Current–voltage curves of the CBM for water-LiCl solution. The curves have been measured by inserting the membranes M1 (□), M2 (◇), M3 (△), and M4 (○) in the intermediate region of the CBM. Solid lines show the calculated results.

Mafé and coworkers[1–3,6] reported the ion flux in bipolar membranes for different bipolar membranes at different temperatures. They used the chemical reaction model to quantify the efficiencies of water splitting. In their papers, the dissociation rate constant of water, k_d, is written in the following form.[6,23,24]

$$k_d = k_d^0 \exp\left[\frac{\alpha F}{RT} E\right] \tag{3}$$

where R is the gas constant, T is the absolute temperature, F is Faraday's constant, E is the electric field, α is a microscopic parameter having the dimension of length, and k_d^0 is the effective dissociation rate constant for water, which results from the protonation–deprotonation reactions of Eq. (1) in the absence of an external electric field. k_d^0 is a function of temperature and can be expressed by the following Arrhenius relationship:

$$k_d^0 = A \exp\left[-\frac{E_a}{RT}\right] \tag{4}$$

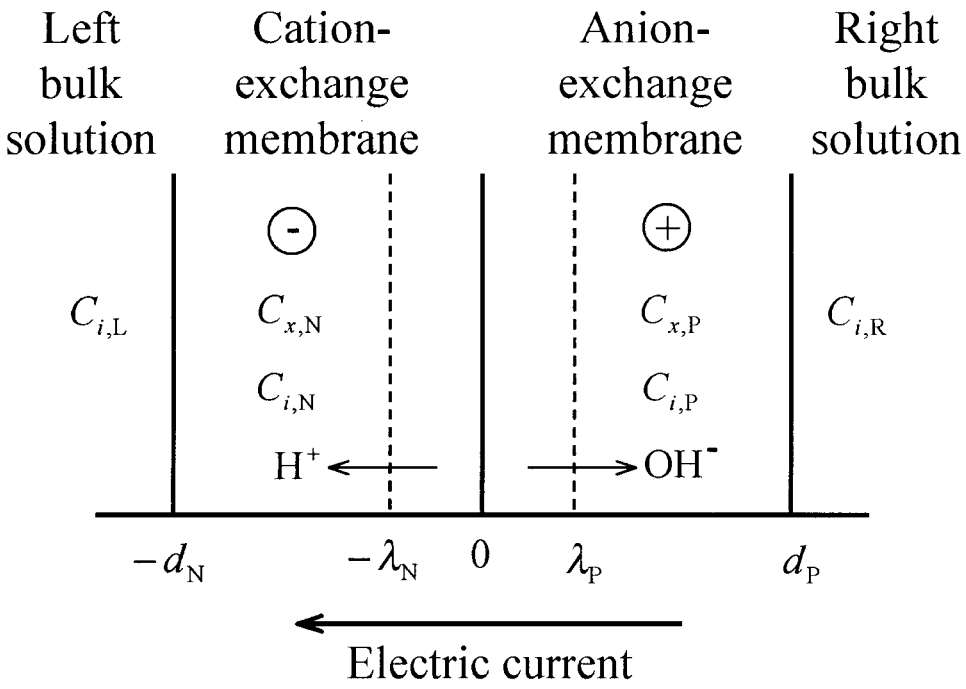

Figure 6 Schematic diagram of the composite bipolar membrane considered under reverse bias conditions. The region from $-\lambda_N$ to λ_P corresponds to the space charge layer.

where A is the preexponential (frequency) factor and E_a is the activation energy of the process.

Figure 6 shows the bipolar membrane separating two solutions of the same uni-univalent electrolyte. The cation-exchange layer extends from $-d_N$ to 0 and has the concentration $C_{x,N}$ of the negatively charged fixed groups. The anion-exchange layer lies between 0 and d_P and has the concentration $C_{x,P}$ of the positively charged fixed groups. The entire system formed by the membrane and the bathing electrolyte solutions is assumed to be isothermal and at a steady state where the solvent flow is neglected. The bias voltage V dependence of the current I, using the space charge model can be written in the form[6]

$$I = (I_{LS} + I_{LW})\left[\exp\left(\frac{FV}{RT}\right) - 1\right] - I_d \qquad (5)$$

where the constants I_{LS} and I_{LW} are defined in the following forms:

$$I_{LS} \equiv F\left[\frac{D_{2,N}C_{2,N}(-d_N)}{d_N} + \frac{D_{1,P}C_{1,P}(d_P)}{d_P}\right] \qquad (6)$$

$$I_{LW} \equiv F\left[D_{3,P}C_{3,P}(d_P)\sqrt{\frac{\chi_P}{D_{3,P}}}\coth\left(d_P\sqrt{\frac{\chi_P}{D_{3,P}}}\right)\right.$$
$$\left. + D_{4,N}C_{4,N}(-d_N)\sqrt{\frac{\chi_N}{D_{4,N}}}\coth\left(d_N\sqrt{\frac{\chi_N}{D_{4,N}}}\right)\right] \qquad (7)$$

and can be interpreted, respectively, as the limiting current densities carried by the salt ions and by the H^+ and OH^- ions generated when no external electric field is applied. $D_{i,K}$ represents the diffusion coefficient of the ith species (i = 1 for salt cations, i = 2 for salt anions, i = 3 for H^+ ions, and i = 4 for OH^- ions) in layer K (K = N and P, which refer to the cationic and anionic layers of the bipolar membrane, respectively), and χ_N and χ_P can be defined by

$$\chi_N \equiv k_r^0 C_{3,N}(-d_N) \qquad (8)$$

$$\chi_P \equiv k_r^0 C_{4,P}(d_P) \qquad (9)$$

where k_r^0 is the recombination rate constant of water when no electric field is applied. $C_{i,K}$ represents the concentration of the ith species in region K (K = L, R, N, and P, which refer to the left and right bulk solutions and to the cationic and anionic layers of the bipolar membrane, respectively) and can be expressed by

$$C_{i,N}(-d_N) = \frac{C_{i,L}}{C_{1,L} + C_{3,L}}\left[\sqrt{\frac{C_{x,N}^2}{4} + (C_{1,L} + C_{3,L})^2 + \frac{(-1)^{i+1}C_{x,N}}{2}}\right] \qquad (10)$$

$$C_{i,\mathrm{P}}(d_{\mathrm{P}}) = \frac{C_{i,\mathrm{R}}}{C_{1,\mathrm{R}} + C_{3,\mathrm{R}}}\left[\sqrt{\frac{C_{x,\mathrm{P}}^2}{4} + (C_{1,\mathrm{R}} + C_{3,\mathrm{R}})^2 + \frac{(-1)^i C_{x,\mathrm{P}}}{2}}\right] \quad (11)$$

The term I_{d} in Eq. (5) is the current density due to the electric field-enhanced water dissociation and can be written in the form

$$I_d \equiv F k_d n \lambda \quad (12)$$

where n is the concentration of active sites in the depleted layer where the reaction is taking place, and k_d is given by Eqs. (3) and (4). The electric field at the junction E and the thickness of the space charge region, λ, are

$$E = \left[\frac{2F}{\varepsilon_r \varepsilon_0}(-V)\frac{C_{x,\mathrm{N}} C_{x,\mathrm{P}}}{C_{x,\mathrm{N}} + C_{x,\mathrm{P}}}\right]^{1/2} \quad (13)$$

$$\lambda \equiv \lambda_{\mathrm{N}} + \lambda_{\mathrm{P}} = \left[\frac{2\varepsilon_r \varepsilon_0}{F}(-V)\frac{C_{x,\mathrm{N}} + C_{x,\mathrm{P}}}{C_{x,\mathrm{N}} C_{x,\mathrm{P}}}\right]^{1/2} \quad (14)$$

where ε_0 is the vacuum electrical permittivity, and ε_r is the dielectric constant.

Although the model was derived by Mafé and coworkers for electrolyte-water solution systems, it can also provide a good fit for the experimental results of the electrolyte-methanol solution systems in this study by adjusting the unknown parameters.[21] The experimental results of the current–voltage curves have been fitted using Mafé's and Ramírez's ion transport theory.[6] According to Bruggeman's equation,[25] the local dielectric constant ϵ_r in the membrane varies only slightly with the dielectric constant of the solvent. Thus, we took the typical value, $\varepsilon_r = 20$, for all of the systems.[26] During the process of parameter estimation, it was found that the value of E_{a} could remain near 30 kJ/mol for all cases, and the values of α could be fixed at 4.1×10^{-10} m and 3.4×10^{-10} m for the solutions of LiCl-water and LiCl-methanol, respectively. Other parameters required in the calculation procedure took the typical values: $D_{i,K} = 10^{-9}$ m^2/s ($i = 1,2, K = \mathrm{N}, \mathrm{P}$) and $D_{i,K} = 10^{-8}$ m^2/s ($i = 3,4, K = \mathrm{N}, \mathrm{P}$). The error caused by these fixed values can be compensated by the regressing process. The parameter nA was taken as an adjustable parameter in this study, and the values of the parameter are given in Table II. The values of parameter nA increase when the solvent splitting effect is enhanced. This result can be explained due to n being the concentration of active sites where the protonation–deprotonation reactions take place; thus it will increase with the increase in active sites in the intermediate region of the CBM. The experimental results show that the electric field-enhanced dissociation reaction occurring in methanol solution is similar to that occurring in water solution, and the existence of functional group will enhance the solvent splitting for both water and methanol.

Table II Values of the Parameters nA and α

Membrane in the Interface of CBM	Water Solution ($\alpha = 4.1 \times 10^{-10}$ m) $nA \times 10^{-8}$ (mol/m^3 s)	Methanol Solution ($\alpha = 3.4 \times 10^{-10}$ m) $nA \times 10^{-8}$ (mol/m^3 s)
Nothing	2.39	1.23
M1	3.40	1.71
M2	3.02	1.53
M3	3.11	1.61
M4	3.15	1.62

CONCLUSIONS

In this study, current–voltage curves were experimentally measured by inserting the thin PAN membrane on the intermediate region of the CBM for water and methanol solutions. The measured results show that the functional group of PAN will increase the water- and methanol-splitting effect, but the effects of Nb_3Ga, C_{60}, and TiO_2 are not obvious. This phenomenon can be explained due to the protonation-deprotonation reactions occurring between the functional group of PAN and the solvent molecules in the intermediate region of the CBM, but similar reactions do not exist between Nb_3Ga, C_{60}, or TiO_2 and the solvent molecules. The experimental results show that the electric field-enhanced dissociation reaction occurring in methanol solution is similar to that occurring in water solution and that the existence of functional group will enhance the solvent splitting for both water and methanol.

REFERENCES

1. Ramírez, P.; Aguilella, V. M.; Manzanares, J. A.; Mafé, S. J Membr Sci 1992, 73, 191.

2. Sokirko, A. V.; Ramírez, P.; Manzanares, J. A.; Mafé, S. Ber Bunsenges Phys Chem 1993, 97, 1040.
3. Ramírez, P.; Rapp, H. J.; Mafé, S.; Bauer, B. J Electroanal Chem 1994, 375, 101.
4. Moussaoui, R. E.; Pourcelly, G.; Maeck, M.; Hurwitz, H. D.; Gavach, C. J Membr Sci 1994, 90, 283.
5. Aritomi, T.; Boomgaard, T.; Strathmann, H. Desalination 1996, 104, 13.
6. Mafé, S.; Ramírez, P. Acta Polymer 1997, 48, 234.
7. Strathmann, H.; Krol, J. J.; Rapp, H. J.; Eigenberger, G. J Membr Sci 1997, 125, 123.
8. Shimizu, K.; Tanioka, A. Polymer 1997, 38, 5441.
9. Higuchi, A.; Nakagawa, T. J Chem. Soc. Faraday Trans 1989, 85, 3609.
10. Higa, M.; Kira, A. J Phys Chem 1995, 99, 5089.
11. Ramírez, P.; Mafé, S.; Manzanares, J. A.; Pellicer, J. J. Electroanal Chem 1996, 404, 187.
12. Tanioka, A.; Shimizu, K.; Miyasaka, H.; Zimmer, J.; Minoura, N. Polymer 1996, 37, 1883.
13. Tanioka, A.; Yokoyama, Y.; Higa, M.; Miyasaka, K. Colloids Surfaces B Biointerfaces 1997, 9, 1.
14. Higa, M.; Tanioka, A.; Kira, A. J Phys Chem B 1997, 101, 2321.
15. Chilcott, T. C.; Coster, H. G. L.; George, E. P. J Membr Sci 1995, 100, 77.
16. Chilcott, T. C.; Coster, H. G. L.; George, E. P. J Membr Sci 1995, 108, 185.
17. Alcaraz, A.; Ramírez, P.; Mafé, S.; Holdik, H. J Phys Chem 1996, 100, 15555.
18. Ohki, S. J Phys Soc Jpn 1965, 20, 1674.
19. Onsager, L. J Chem Phys 1934, 2, 599.
20. Simons, R. Electrochim Acta 1984, 29, 151.
21. Chou, T. J.; Tanioka, A. J Phys Chem B 1998, 102, 7866.
22. Wien, M.; Schile, J. Phys Z 1931, 32, 545.
23. Timashev, S. F.; Kirganova, E. V. Sov Electrochem 1981, 17, 366.
24. Zabolotskii, V. I.; Shel'deshov, N. V.; Gnusin, N. P. Russ Chem Rev 1988, 57, 801.
25. Bruggeman, D. G. A. Ann Physik 1935, 24, 636.
26. Ramírez, P.; Rapp, H. J.; Reichle, S.; Strathmann, H.; Mafé, S. J Appl Phys 1992, 72, 259.